

PAPER • OPEN ACCESS

Charged domain walls in lithium tantalate with compositional gradients produced by partial VTE process

Recent citations

- [Domain-wall engineering and topological defects in ferroelectric and ferroelastic materials](#)
G. F. Nataf *et al*

To cite this article: E D Greshnyakov *et al* 2019 *IOP Conf. Ser.: Mater. Sci. Eng.* **699** 012015

View the [article online](#) for updates and enhancements.

INTERNATIONAL OPEN ACCESS WEEK
OCTOBER 19-26, 2020

ALL ECS ARTICLES. ALL FREE. ALL WEEK.
www.ecsdl.org

**NOW
AVAILABLE**

Charged domain walls in lithium tantalate with compositional gradients produced by partial VTE process

E D Greshnyakov, B I Lisjikh, V I Pryakhina, M S Nebogatikov and V Ya Shur

School of Natural Sciences and Mathematics, Ural Federal University,
620002 Ekaterinburg, Russia

viktoria.pryahina@urfu.ru

Abstract. The morphology of a single charged domain wall, appeared under the action of composition gradients produced by partial VTE procedure by Cherenkov-type second harmonic generation microscopy, was observed in detail. The width of the charged domain wall was estimated as 70 μm . Non-through and through narrow domains, grown from the charged domain wall, were revealed. The maximum length of non-through domains with submicron diameter was about 100 μm . The growth of narrow domains from the charged domain wall was demonstrated and attributed to the action of pyroelectric field. The widening of domains occurred after achieving the polar surface.

1. Introduction

Formation of the initial (as-grown, virgin) domain structure during zero field cooling from the temperature above the transition point in ferroelectric crystals depends on many factors, one of which is a spatial nonuniformity of the material composition [1-5]. Crystal inhomogeneities, such as point defects [6], growth layers [1-3], etc., influence the polarization reversal process due to variations of physical properties and lattice imperfections.

Ferroelectric phase transition in uniaxial crystal without external electric field results in formation of random domain structure, which is determined by spatial distribution of the sign of local built-in fields produced by various defects or concentration gradients [3,4]. It was shown that growth striations oriented perpendicular to the polar axis in lead germanate ($\text{Pb}_5\text{Ge}_3\text{O}_{11}$, PGO) crystals resulted in the formation of charged domain walls [8,9] localized in the points, where the gradient changed its sign [3]. We have shown recently that the single charged domain wall was formed during phase transition in lithium tantalate (LiTaO_3 , LT) with artificially produced composition gradient [10,11].

In our research, we used LT single crystal as a model uniaxial ferroelectric, popular for piezoelectric, electro-optic, pyroelectric, and nonlinear optical applications. LT crystals exist in a wide range of compositions characterized by Li concentration (c_{Li}) ranged from 48.5 to 50 mol.%. Polarization reversal threshold fields [12-14], domain shape [7], and Curie temperature [15,16] depend essentially on composition. The vapour transport equilibration (VTE) procedure, which is mostly used for increasing c_{Li} from congruent CLT (48.5 mol.%) to stoichiometric SLT (50 mol.%) composition [12,13,16], allowed us to create spatially inhomogeneous distribution of c_{Li} by decreasing duration of the procedure. As a result, the LT plates, being stoichiometric at the surfaces and congruent in the bulk, with composition gradient along the polar axis were created [10,11].

As-grown domain structure, appeared due to phase transition during cooling after termination of VTE procedure, depends on the compositional gradient. In the certain range of VTE procedure durations, the



single charged domain wall appeared in the sample centre [10,11]. With advantages of Cherenkov-type second harmonic generation microscopy (CSHG) for imaging domains [17,18] in the crystal bulk, it was possible to obtain the set of domain wall positions at different depths and 3D image of as-grown domain structure.

In this paper, we present the first detail observation of the morphology of single charged domain wall appeared under the action of composition gradients produced by partial VTE procedure.

2. Experimental

2.1. Samples preparation by VTE process

Half-millimetre-thick Z-cut plates of CLT with single-domain initial state were used. During VTE procedure, CLT plate was placed in a crucible with Li-rich powder (60 mol.% Li_2CO_3 + 40 mol.% Ta_2O_5) and was annealed at 1100°C during 40-80 h in high-temperature furnace LHT 01/17 (Nabertherm, Germany). Heating and cooling rates were 1 °C/min.

2.2. Composition measurements

Confocal Raman spectroscopy by means of Alpha 300 AR (WiTec, Germany) was used for a nondestructive measurement of c_{Li} spatial distribution along the polar axis. Since Raman spectrum in LT depends on Li concentration [19, 20], it is possible to evaluate the composition by measuring the full width at half maximum (FWHM) of the 143 cm^{-1} line corresponding to E(TO1) mode. The local c_{Li} value was estimated by $c_{\text{Li}} = 52.04 - 0.3535 \text{ FWHM}$, received from calibrating by homogeneous CLT and SLT plates [11].

2.3. Domain imaging

Optical microscopy (Olympus BX-61, Japan) was used for imaging of the domain structure, revealed by selective etching in HF during about 5 min at room temperature at polar surfaces and Y cross-section. Y cross-section was obtained by cutting VTE-plate and polishing the cut to the optical grade.

Cherenkov-type second harmonic generation (CSHG) was used for non-destructive domain imaging in the bulk with spatial resolution about 500 nm. The measurement setup was realized on the base of Ntegra Spectra (NT-MDT, Russia) using Yb fibre laser (1064 nm, 40 mW).

3. Results and discussion

LT plates with nonuniform spatial distributions of c_{Li} along polar axis were produced by changing the VTE annealing time. Annealing allowed producing LT plates with stoichiometric composition at the polar surfaces and near-congruent in the centre of LT plate. Change of gradient sign (dc_{Li}/dz) in the centre resulted in formation of the single charged domain wall.

The created charged domain wall had a complex morphology with elongated narrow bumps (Fig. 1). Some of bumps reached the polar surfaces. It is clear that 2D cross-section did not allow revealing precise characteristics of 3D domain structure.

CSHG imaging of the domain structure in the bulk allowed to reveal domains between the charged domain wall in the crystal bulk and polar surfaces (Fig. 2). These domains formed as bumps at the charged domain wall and grew in polar direction. Two types of domains have been separated: (1) non-through domains with submicron diameter located in the vicinity of charged domain wall and (2) through domains with diameter below 5 μm reaching the polar surface.

We extracted the area of the reversed polarization from CSHG domain images (Fig. 3). The width of the charged domain wall of the irregular wavy shape was about 70 μm . The total area of submicron non-through domains was negligible compared with through domains, which diameter enlarged after achieving polar surface (completing direct growth). The maximum depth of non-through domains was about 100 μm (Fig. 4). The irregular wavy shape of the charged domain wall can be attributed to a result of the counter motion of the phase boundaries during cooling through the transition point [10, 11]. The narrow domains appeared during subsequent cooling under the action of the pyroelectric field [10, 11].

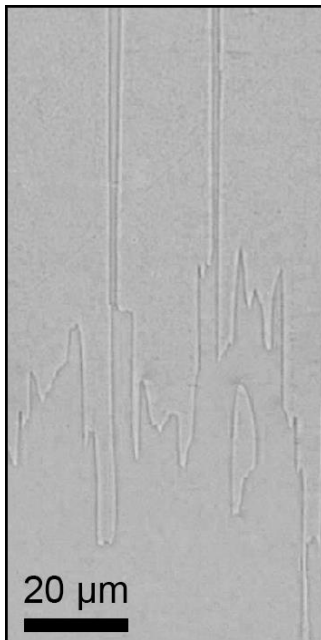


Figure 1. Optical image of domain structure at Y cross-section revealed by selective etching.

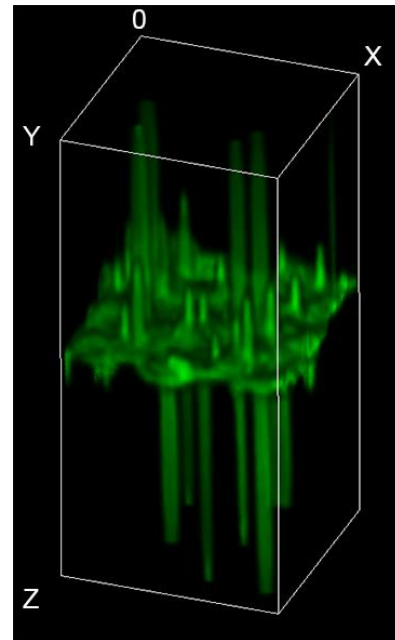


Figure 2. 3D reconstruction of domain structure in the bulk by CSHG imaging. Sizes of volume block XYZ 40×40×500 μm.

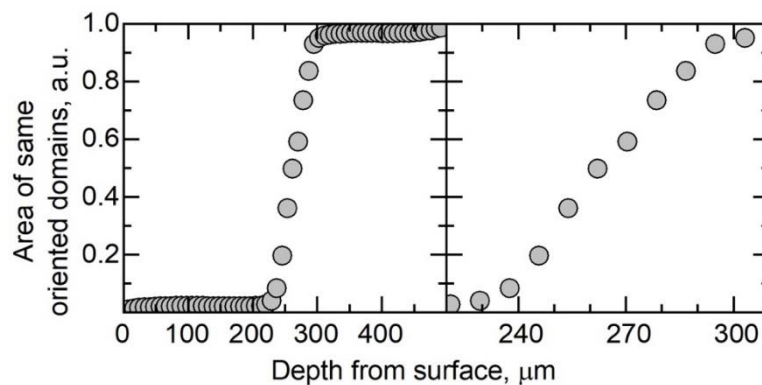


Figure 3. (a) The dependence on the crystal depth of the fraction of the total area of domains with the same orientation. (b) Enlarged region of the charged domain wall.

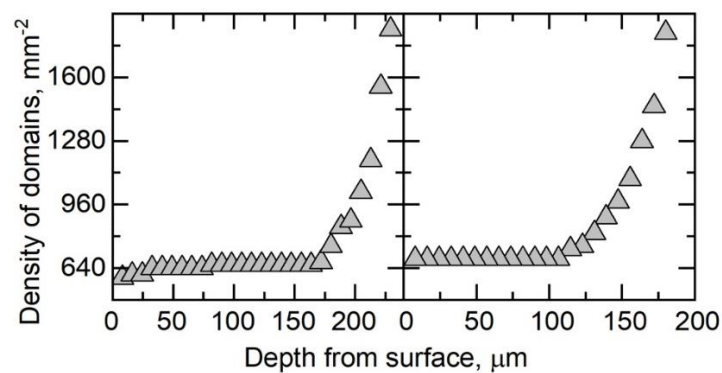


Figure 4. The dependence on the crystal depth of the density of domains appeared between charged domain wall and both polar surfaces.

4. Conclusion

The detail study of the morphology of single charged domain wall appeared under the action of composition gradients produced by partial VTE procedure was realized by Cherenkov-type second harmonic generation microscopy. The width of the charged domain wall was estimated as 70 μm and the maximum length of non-through domains – as 100 μm . The growth of narrow domains from charged domain wall was demonstrated and attributed to the action of the pyroelectric field during cooling. The widening of domains occurred after achieving of polar surfaces.

Acknowledgements

The equipment of Ural Centre for Shared Use “Modern Nanotechnology” Ural Federal University was used. The research was made possible by Russian Science Foundation (project № 19-12-00210).

References

- [1] Shur V Ya, Gruverman A L, Letuchev V V, Rumyantsev E L and Subbotin A L 1989 Domain structure of lead germanate *Ferroelectrics* **98** 29-49
- [2] Shishkin E I, Shur V Ya, Schlaphof F and Eng L M Observation and manipulation of the as-grown maze domain structure in lead germanate by scanning force microscopy *Appl. Phys. Lett.* 2006 **88** 252902
- [3] Shur V and Rumyantsev E 1998 Arising and evolution of the domain structure in ferroics *J. Kor. Phys. Soc.* **32** S727-32
- [4] Kugel V D and Rosenman G 1993 Domain inversion in heat-treated LiNbO_3 crystals *Appl. Phys. Lett.* **62** 2902-4
- [5] Åhlfeldt H 1994 Single-domain layers formed in heat-treated LiTaO_3 *Appl. Phys. Lett.* **64** 3213-5
- [6] Gopalan V, Dierolf V and Scrymgeour D A 2007 Defect-domain wall interactions in trigonal ferroelectrics *Annu. Rev. Mater. Res.* **37** 449-89
- [7] Shur V Ya, Nikolaeva E V, Shishkin E I, Chernykh A P, Terabe K, Kitamura K, Ito H and Nakamura K 2002 Domain shape in congruent and stoichiometric lithium tantalate *Ferroelectrics* **269** 195-200
- [8] Shur V Y, Rumyantsev E L, Nikolaeva E V. and Shishkin E I 2000 Formation and evolution of charged domain walls in congruent lithium niobate *Appl. Phys. Lett.* **77** 3636-8
- [9] Eliseev E A, Morozovska A N, Svechnikov G S, Gopalan V and Shur V Y 2011 Static conductivity of charged domain walls in uniaxial ferroelectric semiconductors *Phys. Rev. B* **83** 235313
- [10] Pryakhina V I, Greshnyakov E D, Lisjikh B I, Akhmatkhanov A R, Alikin D O, Shur V Y and Bartasyte A 2018 As-grown domain structure in lithium tantalate with spatially nonuniform composition *Ferroelectrics* **525** 47-53
- [11] Pryakhina V I, Greshnyakov E D, Lisjikh B I, Nebogatikov M S and Shur V Ya 2019 Influence of composition gradients on heat induced initial domain structure in lithium tantalate *Ferroelectrics* **542** 13-20
- [12] Hum D S, Route R K, Miller G D, Kondilenko V, Alexandrovski A, Huang J, Urbanek K, Byer R L and Fejer M M 2007 Optical properties and ferroelectric engineering of vapor-transport-equilibrated, near-stoichiometric lithium tantalate for frequency conversion *J. Appl. Phys.* **101** 093108
- [13] Tian L, Gopalan V and Galambos L 2004 Domain reversal in stoichiometric LiTaO_3 prepared by vapor transport equilibration *Appl. Phys. Lett.* **85** 4445
- [14] Kitamura K, Furukawa Y, Niwa K, Gopalan V and Mitchell T E 1998 Crystal growth and low coercive field 180° domain switching characteristics of stoichiometric LiTaO_3 *Appl. Phys. Lett.* **73** 3073-5
- [15] Wöhlecke M, Corradi G and Betzler K 1996 Optical methods to characterise the composition and homogeneity of lithium niobate single crystals *Appl. Phys. B Laser Opt.* **63** 323-30
- [16] Bordui P F, Norwood R G, Bird C D and Carella J T 1995 Stoichiometry issues in single-crystal lithium tantalate *J. Appl. Phys.* **78** 4647-50

- [17] Sheng Y, Best A, Butt H-J, Krolikowski W, Arie A and Koynov K 2010 Three-dimensional ferroelectric domain visualization by Čerenkov-type second harmonic generation *Opt. Express* **18** 16539
- [18] Kämpfe T, Reichenbach P, Schröder M, Haußmann A, Eng L M, Woike T and Soergel E 2014 Optical three-dimensional profiling of charged domain walls in ferroelectrics by Čerenkov second-harmonic generation *Phys. Rev. B* **89** 035314
- [19] Kostritskii S M, Aillerie M, Bourson P and Kip D 2009 Raman spectroscopy study of compositional inhomogeneity in lithium tantalate crystals *Appl. Phys. B* **95** 125-30
- [20] Shi L, Kong Y, Yan W, Liu H, Li X, Xie X, Zhao D, Sun L, Xu J, Sun J, Chen S, Zhang L, Huang Z, Liu S, Zhang W and Zhang G 2005 The composition dependence and new assignment of the Raman spectrum in lithium tantalate *Solid State Commun.* **135** 251-6